Available online at www.sciencedirect.com
SCIENCE DIRECT
Journal of Power Sources 156 (2006) 525–532
JOURNAL OF POWER SOURCES
www.elsevier.com/locate/jpowsour

Lithium ion and electronic conductivity in 3-(oligoethylene oxide)thiophene comb-like polymers

David Witker, M. David Curtis *

Department of Chemistry and the Macromolecular Science and Engineering Program, The University of Michigan, Ann Arbor, MI 48109-1055, USA

Received 24 January 2005; received in revised form 13 May 2005; accepted 14 May 2005
Available online 11 July 2005

Abstract

The Li-ion and electronic conductivities of a series of p-doped poly(thiophene)s with oligo-ethylene oxide side chains have been determined at room temperature as functions of side-chain length and concentration of LiOTf dissolved in the polymers in order to assess their utility as binders in Li-ion batteries. The lithium triflate concentration was varied from 0.23 to 2.26 mmol LiOTf/g $-C_2H_4O-$ (100 O:Li to 10 O:Li), and the concentration of dissociated Li^+ was determined from the IR spectra of the polymer solutions. The greatest ionic conductivity, 2×10^{-4} S cm^{-1}, was attained with intermediate concentrations of added salt that corresponded with the greatest degree of LiOTf dissociation. Li-ion mobilities of 5×10^{-7} cm^2 (Vs)$^{-1}$ were measured for poly(thiophene)s (PT) with short oligo(ethylene oxide) side-chains (E_n), PE_2T and PE_3T, whereas the polymers with longer side chains, PE_7T and $PE_{15}T$, had Li-ion mobilities about an order of magnitude greater, 5×10^{-6} cm^2 (Vs)$^{-1}$. The electronic conductivity of the polymers heavily doped with $NOBF_4$ was near 0.1 S cm^{-1} for PE_2T and PE_3T, but was orders of magnitude smaller for the polymers with longer side-chains. Addition of LiOTf caused the electronic conductivity of PE_2T and PE_3T to drop to that of the longer chain polymers whose conductivities were insensitive to the LiOTf concentration.

Keywords: Current collector; Electroactive; Binder; Li ion mobility; Ionic conductor

1. Introduction

In order to achieve high power densities, a battery must be capable of rapid discharge, and this capability requires the electrode structure to have a high electron mobility and that the interface of the electrode with the electrolyte have a high ionic mobility. In the present generation of Li-ion batteries, the electroactive cathode material, e.g., $Li_{(1-x)}CoO_2$, is typically bonded to the current collector plate with a glue, e.g., EPDM, which is an insulator. Thus, some portion of the powdered $Li_{(1-x)}CoO_2$ is isolated from the current collector with resulting loss of capacity. Furthermore, some of the active surface area of the $Li_{(1-x)}CoO_2$ particles is covered by the EPDM, thereby limiting the transport of Li-ions and decreasing the rate of discharge. Therefore, the development of a binder material that can conduct both electrons and Li-ions would appear desirable as a means to improve both the capacity and power density of Li-ion batteries.

Materials that combine the electronic conductivity of conjugated polymers with ion-receptive groups have been studied primarily for use as ion sensors [1–6]. In these applications, ions interact with the ion-coordinating components of the material, leading to changes in the electronic nature of the conjugated polymer backbone. These changes can manifest themselves as differences in the physical properties of the material. Color, fluorescence, electrochemical potential, and conductivity have been used to monitor the concentration of the desired ion in these systems.

Less than 30 years have passed since Wright performed preliminary work on poly(ethylene oxide) (PEO) as an alkali

* Corresponding author. Tel.:+1 734 763 2132; fax: +1 734 763 2307.
E-mail addresses: dwitker@chem.ufl.edu (D. Witker), mdcurtis@umich.edu (M.D. Curtis).

0378-7753/$ – see front matter © 2005 Elsevier B.V. All rights reserved.
doi:10.1016/j.jpowsour.2005.05.060

metal ion conductor [7–9]. The conductivity of PEO-salt solutions is quite temperature dependent. Ionic conduction is facilitated by segmental motion of the flexible PEO chains. Above the melting point, $T_m \approx 65\,^{\circ}C$, values near $10^{-4}\,S\,cm^{-1}$ are observed; but at ambient temperature, the conductivity of these systems is considerably lower. The room temperature conductivity of PEO has been improved through the use of small-molecule plasticizers and the development of less crystalline polymers with PEO side chains (comb polymers) [10–23]. In this work, a series of poly(thiophene)-based comb polymers featuring oligo(ethylene oxide) side chains of various lengths were synthesized, and the conductivities of polymer-salt solutions with several different concentrations of lithium triflate were measured. Ionic conductivity values as great as $2 \times 10^{-4}\,S\,cm^{-1}$ were obtained for the neutral polymer/salt blends. The ionic conductivity of these materials was found to be strongly dependent on the concentration of lithium triflate. The electronic conductivities of the $NOBF_4$-doped polymers were determined also as a function of the LiOTf concentration. Electronic conductivity was observed to drop by several orders of magnitude upon addition of lithium salt.

2. Experimental

All materials used were obtained from Aldrich, Acros, or Fluka and purified according to accepted procedures before use. Standard Schlenk techniques were utilized when air exclusion was necessary. NMR spectra were recorded using a Varian 400 MHz spectrometer. Chemical shifts were referenced to residual solvent.

The monomers, 3-(2,5-dioxahex-1-yl)thiophene (E_1T) and 3-(2,5,8-trioxanon-1-yl)thiophene (E_2T), and their 2-bromo derivatives were synthesized as reported previously [24a,25]. The monomers with longer side chains were synthesized similarly.

Syntheses of 2-bromo-3-(2,5,8,11-tetraoxadodecyl)thiophene (BE_3T), 2-bromo-3-(methoxy(ethoxy)$_{7.5}$)methylthiophene (BE_7T), and 2-bromo-3-(methoxy(ethoxy)$_{15.5}$) methylthiophene ($BE_{15}T$). These monomers were synthesized in the same manner as for the bromination of E_1T [25]. Distillation of the BE_3T product at 0.02 Torr gave a clear liquid boiling from $136-139\,^{\circ}C$. Yield: 83%. ^1H NMR (400 MHz, $CDCl_3$) δ 7.21 (d, $J = 5.8$ Hz, 1H), 6.98 (d, $J = 5.5$ Hz, 1H), 4.45 (s, 2H), 3.59 (m, 10H), 3.32 (s, 3H). BE_7T: this product was purified by flash column chromatography. The stationary phase was neutral alumina and the eluent was ethyl acetate. Volatile contaminants were removed by heating at 100 °C in vacuo for 24 h. Yield: 73%. ^1H NMR (400 MHz, $CDCl_3$) δ 7.18 (d, $J = 5.7$ Hz, 1H), 6.95 (d, $J = 5.5$ Hz, 1H), 4.46 (s, 2H), 3.59 (m, 28H), 3.49 (m, 2H), 3.32 (s, 3H). $BE_{15}T$: this product was also purified by flash chromatography with neutral alumina as the stationary phase and ethyl acetate as the eluent. Volatile contaminants were removed by heating at 100 °C in vacuo for 24 h. Yield: 76%. ^1H NMR (400 MHz, $CDCl_3$) δ 7.24 (d, $J = 6.0$ Hz, 1H), 6.92 (d, $J = 5.5$ Hz, 1H), 4.49 (s, 2H), 3.64 (m, 50H), 3.52 (m, 2H), 3.37 (s, 3H).

The polymers were prepared by McCullough's GriM method with only minor changes to the reported syntheses for PE_nT ($n = 1,2$) [24,26]: Regioregular poly(3-(2,5,8,11-tetraoxadodecyl)thiophene) (PE_3T). Yield: 29%. ^1H NMR (400 MHz, $CDCl_3$) δ 7.20 (s, 1H), 4.58 (s, 2H), 3.64 (m, 10H), 3.49 (m, 2H), 3.31 (s, 3H). Regioregular poly(3-(methoxy(ethoxy)$_{7.5}$)methylthiophene) (PE_7T). The fraction of the product soluble in methanol was recovered and purified by precipitation with hexanes. Yield: 42%. ^1H NMR (400 MHz, MeOH-d^4) δ 7.25 (s, 1H), 4.65 (s, 2H), 3.68 (m, 28H), 3.54 (m, 2H), 3.33 (s, 3H). Regioregular poly(3-(methoxy(ethoxy)$_{15.5}$)methylthiophene) ($PE_{15}T$). The fraction of the product soluble in methanol was recovered and purified by precipitation with hexanes. Yield: 40%. ^1H NMR (400 MHz, MeOH-d^4) δ 7.21 (s, 1H), 4.61 (s, 2H), 3.62 (m, 50H), 3.50 (m, 2H), 3.29 (s, 3H). No signals due to H-atoms at the ends of the chains were detected above the noise level ($\leq$1/20 of the peak height for the ring H-atom) for any of the polymers reported here, indicating the degree of polymerization, DP $\geq$ 20.

All current/voltage measurements were performed using a Perkin-Elmer model 273A potentiostat in conjunction with a PC interface for data acquisition. Film thickness was measured by profilometry using a Dektak [3] profilometer. DSC scans were performed with a Perkin-Elmer DSC 7 calorimeter at $5\,^{\circ}C\,min^{-1}$.

2.1. Infrared spectra

IR spectra were obtained from KBr pellets using a Perkin-Elmer Spectrum BX spectrometer. Deconvolution of infrared peaks was accomplished with GRAMS/32 software. The peaks were assumed to be of Lorentzian shape. The area of the signal corresponding to the symmetric sulfur–oxygen stretch of the triflate ion was normalized by referencing it to the area of the peak for the carbon–hydrogen stretching mode observed near $3000\,cm^{-1}$. In order to relate the area of each component peak to the concentration of the ionic species it represents, the spectra of the most dilute PE_nT/LiOTf blends were considered. In these cases, essentially all of the lithium triflate was dissociated, as indicated by curve-fitting. So, the ratio of the area of the observed peak to the total salt concentration was indicative of the oscillator strength of the free triflate ion. This ratio was then applied to samples with intermediate LiOTf concentrations which showed free ions and ion pairs. The peak area corresponding to free ions was converted to concentration and then subtracted from the total salt concentration. In this way, the ratio of peak area to ion pair concentration was determined. The procedure was then repeated for the spectra of the most concentrated samples, allowing for the concentration of multiple-ion aggregates to be determined.

2.2. Ionic conductivity

Samples for ionic conductivity determinations were prepared by dissolving 100 mg of each polymer in a solvent. Chloroform was used for PE_2T and PE_3T, while methanol was used to dissolve PE_7T and $PE_{15}T$. Each solution was divided into five equal portions. A solution of lithium triflate in acetonitrile for the short side chain polymers ($n = 2,3$) or in methanol for the long side chain materials ($n = 7,15$) was added to give samples with oxygen to lithium ratios of 10 (2.27 mmol LiOTf/g $-C_2H_4O-$), 20 (1.14 mmol LiOTf/g $-C_2H_4O-$), 30 (0.76 mmol LiOTf/g $-C_2H_4O-$), 50 (0.45 mmol LiOTf/g $-C_2H_4O-$), and 100 (0.23 mmol LiOTf/g $-C_2H_4O-$). Each solution was then cast into two films. The films were dried at 0.05 Torr at room temperature for 24 h before taking measurements on them. After vacuum drying, the film samples were moved into an argon atmosphere drybox. PE_1T was observed to precipitate from the chloroform solution upon addition of very minute volumes of the salt solution in acetonitrile as well as other solvents. The failure of this polymer to remain in solution resulted in a suspension from which uniform films could not be obtained, and ionic conductivity determinations for PE_1T were not obtained.

The potential was scanned from −100 to 100 mV at 1 mV s^{-1} to generate the current/voltage curves for the determination of ionic conductivity. These limits were selected to maximize the current observed while keeping the potentials low enough so that no oxidation or reduction of the material could occur. Only the movement of charge carriers would thus contribute to the observed current. Several samples were analyzed with a stepwise application of potential. Voltages from −50 to 50 mV in steps of 10 mV were applied for sixty seconds and the current was recorded for each.

2.3. Electronic conductivity

Polymer samples doped with $NOBF_4$ were handled under a dry nitrogen atmosphere until after doping and drying. To dope samples with $NOBF_4$, 300 mg of each polymer was dissolved or swelled in dry acetonitrile. Then, the solution was separated into six equal portions and the appropriate amount of a lithium triflate solution in acetonitrile was added to produce samples with [O]:[Li] ratios of 10, 20, 30, 50, and 100 as well as a salt-free sample. These polymers were then doped in solution by introduction of $NOBF_4$ in dry acetonitrile. One equivalent $NOBF_4$ was used for every two monomer units. The resulting dark blue suspensions were then stirred at room temperature for 60 min. After this time, the solvent was removed in vacuo. The dry materials were collected and pressed into pellets at 10,000 psi. The resulting pellets were immediately placed into the measurement cell, equipped with two stainless steel electrodes, and used to collect current/voltage data in the range 0–100 mV in 10 mV steps. Two pellets of each material were produced and the results for the two were averaged.

3. Results and discussion

The polymers used in this study were synthesized by the methods developed by McCullough et al. (Scheme 1) [24,26]. This approach gives materials that are highly regioregular with nearly 100% head-to-tail linkages. Also, defects such as mislinked rings and cross-links that are formed during oxidative polymerizations are eliminated. ^1H NMR spectroscopy showed no evidence of significant head-to-head coupling or irregular linkages in the polymers prepared in this study. The polymer with the shortest side-chain, PE_1T, was soluble only in chlorinated solvents, while PE_2T and PE_3T were soluble in a wide variety of organic solvents. The compounds with longer side-chains, PE_7T and $PE_{15}T$, were soluble only in polar solvents such as acetone, methanol, or even water.

3.1. Ionic conductivity

Samples for ionic conductivity determinations were prepared by dissolving measured amounts of polymer and

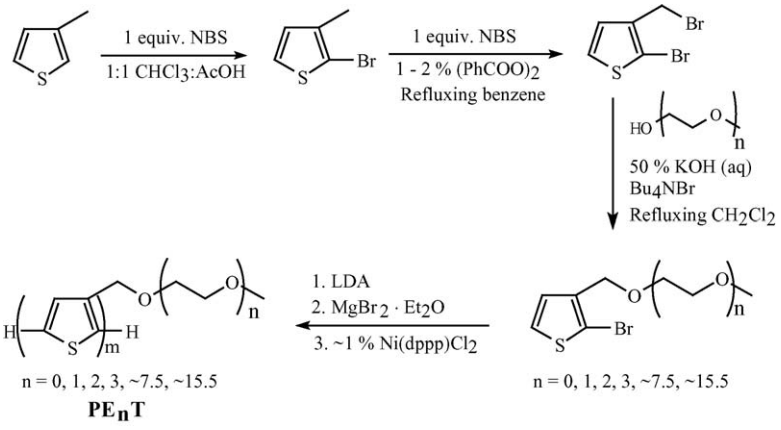

Scheme 1.

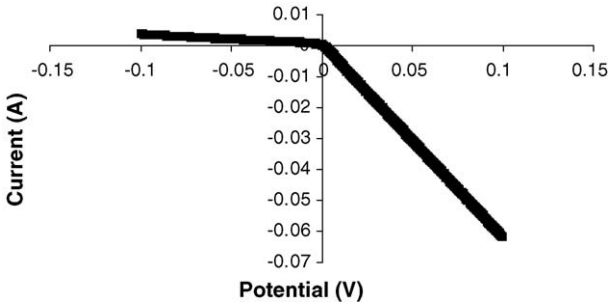

Fig. 1. Typical current/voltage profile of the PE_nT/LiOTf series of materials.

lithium triflate in an appropriate solvent, and films of the polymer/salt blend were cast onto stainless steel plates. The addition of solutions of lithium triflate in acetonitrile to chloroform solutions of PE_1T led to precipitation of the polymer and prevented the casting of uniform films of this material. Due to this difficulty, ionic conductivity determinations on PE_1T were not performed. However, the remaining polymer/LiOTf blends formed excellent films before doping with $NOBF_4$ (see below). After casting and solvent-annealing, the polymer/salt films were loaded into a conductivity cell fitted with one blocking and one non-blocking (Li) electrode [27,28]. In this type of apparatus, positive potentials applied at the stainless steel contact will induce electronic charge carriers to migrate through the sample. When the bias is reversed, both Li-ion and electronic charge carriers migrate across the polymer. Because of the contribution of the ionic charge carriers, the current measured when the Li-electrode is biased positive (anodic) is greater than that observed with the opposite applied bias (Fig. 1). From the measured *I–V* data, along with the physical dimensions of the sample, the ionic conductivity can be calculated as $\sigma_{\text{ionic}} = (d/A)[(I/V)_{\text{anodic}} - (I/V)_{\text{cathodic}}]$, where d = sample thickness, A = sample area.

When plotted as a function of total LiOTf concentration, the ionic conductivity of the materials showed maxima at intermediate lithium triflate concentrations (Fig. 2). The maximum ionic conductivity for PE_2T occurred at an oxygen-to-lithium ratio of 20:1 (1.13 mmol LiOTf/g $–C_2H_4O–$). For all of the other polymers examined, the maximum ionic conductivity was found at [O]:[Li] = 30:1 (0.75 mmol LiOTf/g $–C_2H_4O–$). Conductivity is given by $\sigma = nq\mu$ and is thus

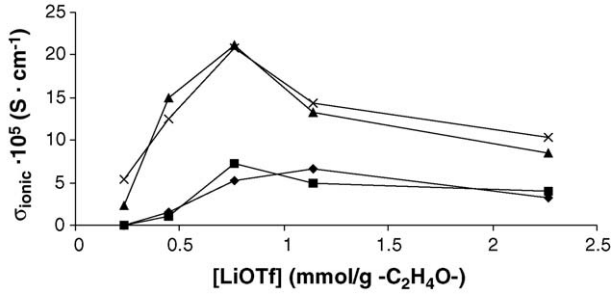

Fig. 2. Ionic conductivity of the PE_nT/LiOTf series as a function of total LiOTf added. (♦) PE_2T; (■) PE_3T; (▲) PE_7T; (×) $PE_{15}T$.

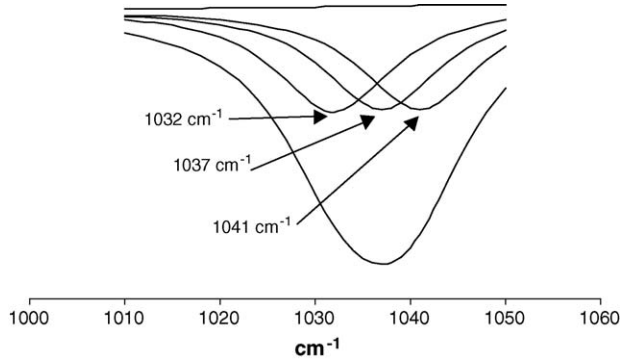

Fig. 3. Deconvolution of the signal corresponding to the symmetric sulfur–oxygen stretch of the triflate ion. Signals for free ions (1032 cm^{-1}), ion pairs (1037 cm^{-1}), and multiple-ion aggregates (1041 cm^{-1}) are shown.

dependent on the concentration, charge, and mobility of the mobile charge carriers. The effective concentration of carriers is given by, $n = f[\text{LiOTf}]_{\text{total}}$, where f = degree dissociation of the LiOTf into "free" lithium and triflate ions. The degree of dissociation was determined from the absorption peaks corresponding to the symmetric sulfur–oxygen stretch in the IR spectra of the LiOTf/polymer solutions. It has been reported previously that this mode appears at 1032 cm^{-1} for free triflate ions, at 1037 cm^{-1} for ion pairs, and at 1041 cm^{-1} for multiple-ion aggregates [26,29]. A typical deconvolution of the sulfur–oxygen stretching peak is shown in Fig. 3. The peak areas were corrected for differences in oscillator strength and the fraction of dissociated LiOTf was determined from the corrected areas, $f = A_{1032}/\Sigma A_i$, where A_{1032} is the corrected area of the 1032 cm^{-1} peak. Essentially all of the lithium triflate was dissociated at concentrations less than about 0.75 mmol LiOTf/g $–C_2H_4O–$, regardless of the length of the side chains. That is, the charge carrier concentration was equivalent to the total salt concentration. Above 0.75 mmol LiOTf/g $–C_2H_4O–$, the concentration of free lithium triflate decreased as the total salt concentration increased (Fig. 4a), and the concentration of associated ions increased (Fig. 4b). These data support the finding that ionic conductivity in these systems is greatest at intermediate salt concentrations.

In addition to charge carrier concentration, ionic conductivity is also proportional to the ion mobility. While it is true that the mobility is higher above the glass transition temperature, T_g, or melting point, T_m, in a given polymer matrix, a comparison of T_m or T_g of different materials cannot be used to predict relative mobilities in the different media, even though it is often assumed that materials with higher values of T_g are more rigid than those with lower glass transitions. This rigidity translates into decreased segmental motion of the PEO components and lower ionic mobility. However, this assumption is not necessarily true for polymers with glass transition temperatures well below 25 °C. The behavior of the materials at sub-ambient temperatures may not be an accurate indicator of their stiffness at a considerably more elevated temperature. Nevertheless, the glass transition tem-

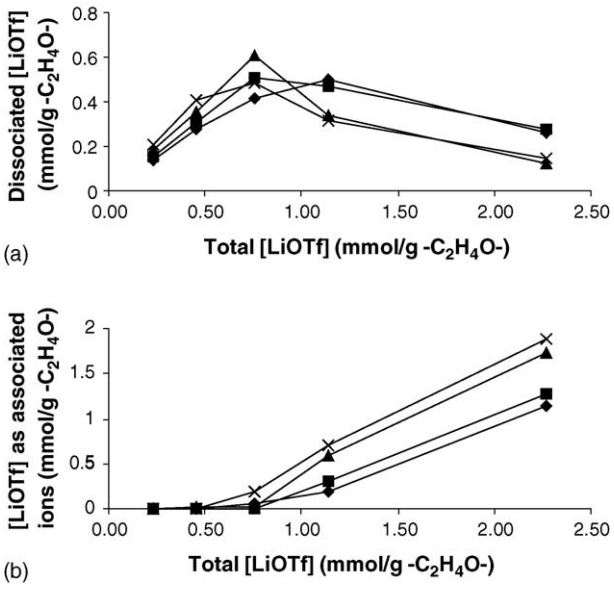

Fig. 4. (a) Concentration of dissociated lithium triflate as a function of concentration in the PE_nT/LiOTf series. (b) Concentration of associated lithium triflate ions (ion pairs plus multiple-ion aggregates). (♦) PE_2T, (■) PE_3T, (▲) PE_7T, (×) $PE_{15}T$.

perature of each polymer/salt blend was determined in order to shed some light on the ionic mobility of lithium ions in these systems.

Usually, glass transition temperatures of salt/polymer solutions tend to increase with increasing salt concentration [30–34]. This effect is usually attributed to the formation of transient cross-links formed by association of PEO chains on different segments with Li^+ ions in the polymer matrix. The DSC scans of the polymer/salt solutions investigated here showed a rather different trend. The PE_nT polymers with relatively short side chains ($n = 2,3$) had maxima in their T_g values at intermediate salt concentrations, whereas those polymers with longer side chains ($n = 7,15$) displayed a monotonic decrease in T_g with increasing salt concentration (Fig. 5). These results may be explained by considering the effect that ion association exerts on T_g. Ions present as ion pairs or multiple-ion aggregates will not be coordinated to the PEO-like side chains as strongly as those that are dissociated. As ion association increases with increasing total salt

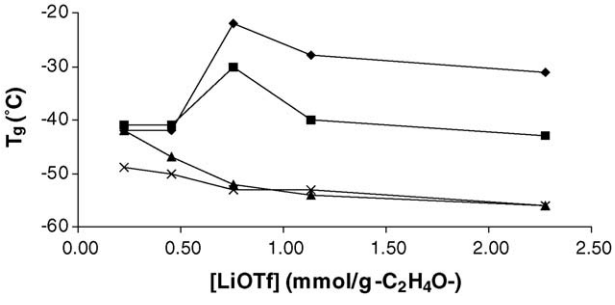

Fig. 5. Glass transition temperatures of the PE_nT series as a function of lithium triflate concentration. (♦) PE_2T, (■) PE_3T, (▲) PE_7T, (×) $PE_{15}T$.

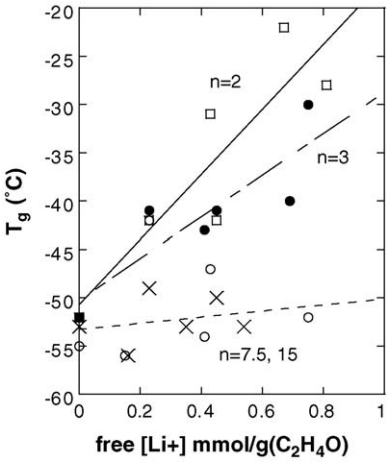

Fig. 6. Glass transition temperatures of PE_nT/LiOTf blends as a function of free lithium ion concentration. (□) PE_2T, (●) PE_3T, (◯) PE_7T, (×) $PE_{15}T$.

concentration, less free lithium ions are available to stiffen the polymer. As Fig. 6 shows, there is only a poor correlation of T_g with the free lithium ion concentration. The lack of a strict correlation of T_g with a single parameter, e.g., the concentration of free lithium ion, is not surprising, as the presence of ion pairs and multiple-ion aggregates will most likely affect the glass transition temperatures. In fact, for each polymer studied, all those that have glass transition temperatures more than 2 °C below the fitted lines in Fig. 6 contain a significant concentration of associated ions. That is, these samples are those with a high total salt concentration. This result suggests that ion pairs and multiple-ion aggregates have the effect of lowering glass transitions just as free ions act to raise T_g. Values of T_g rise as salt is added to the pristine polymer until the point of associated ion formation is reached. Then, partially due to the observed decrease in free ion concentration and partially to the formation of ion pairs and multiple-ion aggregates, values of T_g drop as the total salt concentration increases. One also notes that the T_gs of the polymers with the shorter side chains are more sensitive to the concentration of free ions (larger slopes in Fig. 6).

An estimate of ionic mobility can be obtained by considering the relationship between ionic conductivity and charge carrier concentration. Fig. 7 shows that there is a linear correlation of the ionic conductivity as a function of free Li-ion concentration ($R \sim 0.92$). At steady state, any polarization current has decayed and the measured current is due solely to the mobility of the Li-ions. (Note: The triflate ions do not contribute to the steady-state current because there is no source of triflate ions; the choice of electrodes is "blocking" for triflate, but not for Li^+.) The slopes of these plots are directly proportional to the Li-ion mobility (μ = slope/Ne). The average ionic mobility so obtained ranged from 1.8×10^{-4} ($n = 2$) to 3.8×10^{-4} cm^2 $(Vs)^{-1}$ ($n = 15$). The slightly higher mobility of the polymers with the longer side chains is probably due to the presence of a higher proportion of the ion-receptive components in these materials. PE_7T and $PE_{15}T$ are more like

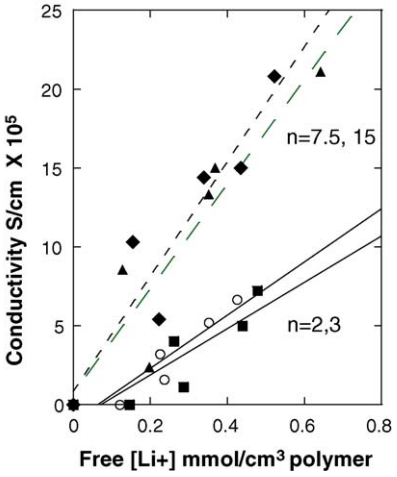

Fig. 7. Ionic conductivity of the PE_nT/LiOTf blends as a function of free ion concentration. (◯) PE_2T, (■) PE_3T, (▲) PE_7T, (♦) $PE_{15}T$.

simple PEO than are their short-side-chain counterparts that contain a higher proportion of non-ionic conductive polythiophene backbone.

From the results described here, it seems that ionic conductivity in these systems is governed primarily by the concentration of available charge carriers. No great enhancement of ionic mobility is gained by varying the length of the ion-conducting side chains.

3.2. Electronic conductivity of p-doped, salt-free polymers

The PE_nT polymers were heavily doped with $NOBF_4$ in order to simulate the level of oxidation expected for the polymers in equilibrium with a fully charged cathode in a Li-ion battery (ca. 4 V versus Li/Li^+). Because the heavy doping rendered the polymer films brittle with or without the addition of LiOTf, electronic conductivities of the doped polymers were measured on pressed pellets of the doped-polymer/LiOTf blends. The current/voltage curves of the $NOBF_4$-doped, LiOTf-free polymer pellets were linear, indicating that no electrochemical reactions were occurring in the potential range used. When the current was applied in steps, there was no variation in the current with time, indicating the absence of polarization contributions to the conductivity. The conductivities were determined from the slopes of the *I/V* curves and are presented in Fig. 8. The conductivities of the doped polymers with short side-chains were in the range, 0.1–0.2 S cm^{-1}, but fell to 3×10^{-6} S cm^{-1} for $PE_{15}T$. X-ray analysis of the doped polymer films showed no evidence for crystallinity, so we attribute the decreased conductivity of the polymers with longer side-chains to the simple dilution of the electroactive main-chain by the insulating side-chains, thus increasing the inter-chain hopping barrier. The conductivities that we measure for PE_1T and PE_2T are considerably less than those determined by McCullough et al. for I_2-doped films [24]. We ascribe the lower conductivities to the fact that

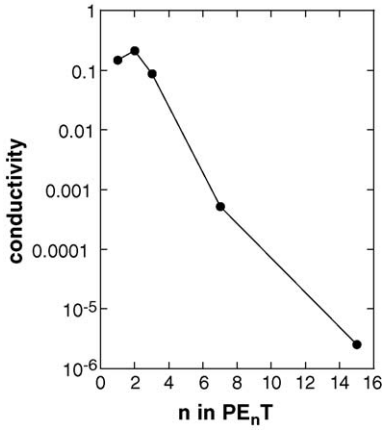

Fig. 8. Electronic conductivity of the PE_nT series doped with $NOBF_4$ as a function of side-chain length.

the measurements were made on pressed pellet samples with the two-point probe technique. The increased level of oxidation in the $NOBF_4$-doped polymers, as compared to the iodine-doped samples, may also contribute to the decrease in the conductivity by decreasing the concentration of neutral hopping sites required for the redox-type conductivity.

3.3. Electronic conductivity of polymer/salt blends

The addition of lithium triflate to the p-doped (oxidized) polymer samples was observed to dramatically decrease the electronic conductivity of the samples, as was observed in work directed towards sensor applications [35–38]. Whereas the doped PE_nT materials with short side chains ($n = 2,3$) showed conductivities on the order of 10^{-1} S cm^{-1} in their salt-free states, polymers with added LiOTf were four to five orders of magnitude less conductive. Furthermore, resistance measurements performed on the PE_nT/LiOTf blends also revealed significant polarization upon initial application of a potential (Fig. 9). This current–time curve indicates that

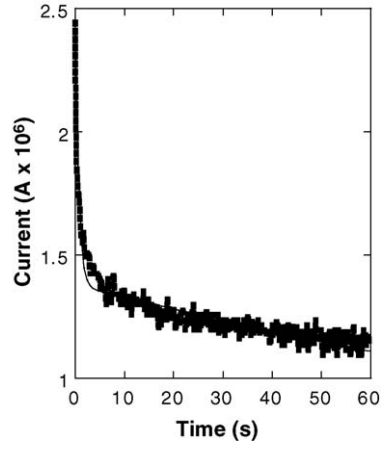

Fig. 9. Current vs. time for PE_2T/LiOTf [O]:[Li] = 10, showing the effect of polarization current. The thin line is a double exponential fit (see text).

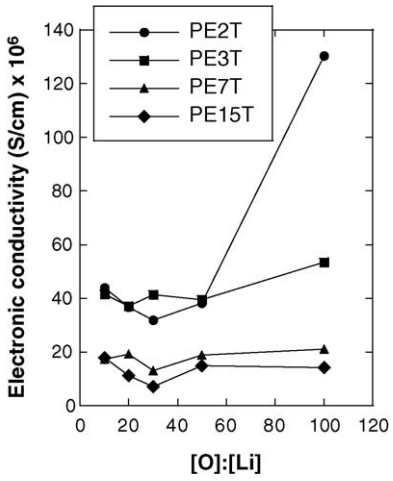

Fig. 10. Effect of lithium salt concentration on electronic conductivity.

a significant percentage of the initial current is due to ionic motion rather than electronic current. The curve was fitted to a double exponential ($R = 0.95$, $\chi^2 = 0.559$) with two quite different relaxation times: 0.71 and 278 s. These times may represent contributions from drift motions of the ions and polymer chains, respectively. The difference in polarization currents between the oxidized polymer/salt blends and the LiOTf-free samples is most likely due to the greater conductivity of the salt-free materials as compared to the blends. In salt-free samples, which are much more electronically conductive than the blends, the electronic current is so great that the contribution of the polarization currents is insignificant. Because of the polarization effects, it was necessary to use stepwise applications of potential for the determination of each sample's electronic resistance. The current was allowed to stabilize at each voltage before the current was recorded.

The conductivities of the doped, salt-polymer blends are shown in Fig. 10 as a function of chain length and salt concentration. The values are in the range 10–40 $\mu S\,cm^{-1}$, except for the polymer with the shortest side-chain, PE_2T, which starts to show an increase in conductivity at the lowest salt concentration studied. Otherwise, changes in the salt concentration have little effect on the conductivities in the concentration range studied here. The conductivities of the doped PE_2T and PE_3T polymer/salt blends are nearly five orders of magnitude below those of the salt-free polymers. The decrease in electronic conductivity may be caused by pinning of the holes in the PT chain by the added triflate anions and/or to twisting of the PT backbone caused by coordination of the Li^+ ions to the PEO sidechains. In contrast, $PE_{15}T$, the least conductive polymer in its salt-free state ($2.5\ \mu S\,cm^{-1}$) experiences a slight increase in conductivity upon salt addition. These results also suggest that there is a lower limit for the conductivity of these materials. The retarding effect of electrostatic interactions between the added ions and the mobile (electron) holes appears to reach a saturation level at the salt concentrations studied.

4. Conclusions

A series of comb-like poly[3-(oligoethylene oxide)thiophene]s were explored for use as lithium ion conductors. At loadings of lithium triflate higher than about 0.75 mmol LiOTf/g $-C_2H_4O-$, ion pairs and multiple-ion aggregates were formed, and the concentration of free lithium ions, which are the primary ionic charge carriers in these systems, decreased. The ionic conductivity of these materials is proportional to the concentration of free Li-ions and reaches a maximum at intermediate concentrations of LiOTf. Values as high as $2 \times 10^{-4}\ S\,cm^{-1}$ were observed. The lithium ion mobilities range between 2 and $3 \times 10^{-4}\ cm^2\,(Vs)^{-1}$.

The electronic conductivity of polymers that were heavily doped with $NOBF_4$ was extremely sensitive to the length of the side chains. The polymers with shorter side chains had conductivities near $0.1\ S\,cm^{-1}$, whereas the conductivity of polymers with longer side chains was in the range of $2\ \mu S\,cm^{-1}$. The addition of lithium triflate to the polymer samples caused the electronic conductivity of the shorter side-chain polymers to decrease to the same level as observed for the pristine long side-chain materials.

The poor film-forming ability of the heavily doped polymers reported here precludes their use as binders in lithium ion batteries. Batteries are usually assembled in their discharged state, and, in their neutral state, the longer side-chain polymers form good films that are able to fasten the active cathode material to the current collector. However, when the cell is charged the polymeric binder would be oxidized, and films of the oxidized polymers tend to crack and peel. This effect would most likely cause the cathode material to become detached from the current collector after several charge/discharge cycles, ultimately leading to cell failure. However, this work does serve as a starting point for the development of electroactive binders for lithium ion batteries. Future efforts will be necessary to determine methods to simultaneously optimize both electronic and ionic conductivity while maintaining film quality during cell cycling.

Acknowledgments

The authors thank Dr. A. Nazri for helpful suggestions. Partial support for this research was provided by the US Department of Energy through a subcontract from the Lawrence Berkeley National Laboratory, contract #6455828.

References

[1] D.T. McQuade, A.E. Pullen, T.M. Swager, Chem. Rev. 100 (2000) 2537.
[2] L.H. Shi, F. Garnier, J. Roncali, Synth. Met. 41–43 (1991) 547.
[3] P.N. Bartlett, A.C. Benniston, L.-Y. Chung, D.H. Dawson, P. Moore, Electrochim. Acta 36 (1991) 1377.

[4] H.K. Youssoufi, M. Hmyene, F. Garnier, D. Delabouglise, J. Chem. Soc. Chem. Commun. (1993) 1550.
[5] F. Garnier, H. Korri, M. Hmyene, A. Yassar, Polym. Prepr. 35 (1994) 205.
[6] H.K. Youssoufi, A. Yassar, S. Baïteche, M. Hmyene, F. Garnier, Synth. Met. 67 (1994) 251.
[7] P.V. Wright, Br. Polym. J. 7 (1975) 319.
[8] P.V. Wright, J. Polym. Sci., Polym. Phys. Ed. 14 (1976) 955.
[9] D.E. Fenton, J.M. Parker, P.V. Wright, Polymer 14 (1973) 589.
[10] I.E. Kelly, J.R. Owen, B.C.H. Steele, J. Electroanal Chem. 168 (1984) 467.
[11] I.E. Kelly, J.R. Owen, B.C.H. Steele, J. Power Sources 14 (1985) 13.
[12] M.Z.A. Munshi, B.B. Owens, Solid State Ionics 26 (1988) 41.
[13] M.H. Sheldon, M.D. Glasse, R.J. Latham, R.G. Linford, Solid State Ionics 34 (1989) 135.
[14] D.W. Xia, D. Soltz, J. Smid, Solid State Ionics 14 (1984) 221.
[15] P.M. Blonsky, D.F. Shriver, P. Austin, H.R. Allcock, Solid State Ionics 18/19 (1986) 258.
[16] P.M. Blonsky, D.F. Shriver, P. Austin, H.R. Allcock, J. Am. Chem. Soc. 106 (1984) 6854.
[17] Y. Yamaguchi, S. Aoki, M. Watanabe, K. Sanui, N. Ogata, Solid State Ionics 40/41 (1990) 628.
[18] D. Fish, I.M. Khan, J. Smid, Makromol. Chem., Rapid Commun. 7 (1986) 115.
[19] K. Inoue, H. Miyamoto, T. Itaya, J. Polym. Sci. A: Polym. Chem. 35 (1997) 1839.
[20] H.R. Allcock, R. Ravikiran, S.J.M. O'Connor, Macromolecules 30 (1997) 3184.
[21] E.A. Rietman, M.L. Kaplan, J. Polym. Sci. C: Polym. Lett. 28 (1990) 187.
[22] M. Yoshizawa, H. Ohno, Electrochim. Acta 46 (2001) 1723.
[23] Z.-U. Yang, L. Wang, N.E. Drysdale, M. Doyle, Macromolecules 36 (2003) 8205.
[24] (a) R.D. McCullough, S.P. Williams, S. Tristram-Nagle, M. Jayaraman, P.C. Ewbank, L. Miller, Synth. Met. 69 (1995) 279;
(b) R.D. McCullough, S.P. Williams, J. Am. Chem. Soc. 115 (1993) 11608.
[25] C.V. Pham, H.B. Mark Jr., H. Zimmer, Synth. Commun. 16 (1986) 689.
[26] R.S. Loewe, P.C. Ewbank, J. Liu, L. Zhai, R.D. McCullough, Macromolecules 34 (2001) 4324.
[27] C.J. Hawker, F. Chu, P.J. Pomery, D.J.T. Hill, Macromolecules 29 (1996) 3831.
[28] G.-A. Nazri, Solid State Ionics 34 (1989) 97.
[29] M. Kakihana, S. Schantz, L.M. Torell, J.R. Stevens, Solid State Ionics 40/41 (1990) 641.
[30] S. Schantz, J. Sandahl, L. Börjesson, L.M. Torell, Solid State Ionics 28/30 (1988) 1047.
[31] M.A. Ratner, D.F. Shriver, Chem. Rev. 88 (1988) 109.
[32] P.M. Blonsky, D.F. Shriver, P. Austin, H.R. Allcock, J. Chem. Am. Soc. 106 (1984) 6854.
[33] K. Inoue, H. Miyamoto, T. Itaya, J. Polym. Sci. A: Polym. Chem. 35 (1997) 1839.
[34] D. Fish, I.M. Khan, J. Smid, Makromol. Chem., Rapid Commun. 7 (1986) 115.
[35] G.-A. Nazri, Mater. Res. Soc. Symp. Proc. 135 (1989) 117.
[36] J.J. André, M. Bernard, B. François, C. Mathis, J. Phys. 44 (1983) 3–19.
[37] P. Bäuerle, G. Götz, M. Hiller, S. Scheib, T. Fischer, U. Segelbacher, M. Bennati, A. Grupp, M. Mehring, M. Stoldt, C. Seidel, F. Geiger, H. Schweizer, E. Umbach, M. Schmelzer, S. Roth, H.J. Egelhaaf, D. Oelkrug, P. Emele, H. Port, Synth. Met. 61 (1993) 71.
[38] P. Bäuerle, S. Scheib, Adv. Mater. 5 (1993) 848.